



# Effect of grain size of primary $\alpha$ phase on bonding interface characteristic and mechanical property of press bonded Ti–6Al–4V alloy

Hong LI<sup>1,2</sup>, Miao-quan LI<sup>1,2</sup>, Hong-bin LIU<sup>2</sup>, Chao ZHANG<sup>2</sup>

1. State Key Laboratory of Solidification Processing, Northwestern Polytechnical University, Xi'an 710072, China;
2. School of Materials Science and Engineering, Northwestern Polytechnical University, Xi'an 710072, China

Received 16 March 2015; accepted 26 August 2015

**Abstract:** The effect of grain size of primary  $\alpha$  phase on the bonding interface characteristic and shear strength of bond was investigated in the press bonding of Ti–6Al–4V alloy. The quantitative results show that the average size of voids increases from 0.8 to 2.6  $\mu\text{m}$  and the bonding ratio decreases from 90.9% to 77.8% with an increase in grain size of primary  $\alpha$  phase from 8.2 to 16.4  $\mu\text{m}$ . The shape of voids changes from the tiny round to the irregular strip. The highest shear strength of bond can be obtained in the Ti–6Al–4V alloy with a grain size of 8.2  $\mu\text{m}$ . This is contributed to the higher ability of plastic flow and more short-paths for diffusion in the alloy with smaller grain size of primary  $\alpha$  phase, which promote the void closure process and the formation of  $\alpha/\beta$  grains across bonding interface.

**Key words:** grain size; bonding interface; void closure; shear strength; press bonding; Ti–6Al–4V alloy

## 1 Introduction

Titanium alloy has a variety of excellent physical and mechanical properties, which include high specific strength, good corrosion resistance and superior heat resistance [1,2]. It has been used to manufacture the lightweight components for aircraft. Press bonding is an effective and precise bonding method for titanium alloy, by which a bond with aspired microstructure and mechanical properties comparable to that of base alloy can be obtained in a short time [3]. As one of the solid state bonding method, it is suitable to bonding the components with complex inner structure.

The performance of press bonded components is mainly dependent on the microstructure and mechanical property of bond, which is controlled by two processes including the void closure and metallurgical bonding. In these two processes, the mass transfer is driven by the plastic flow and atom diffusion, which is significantly influenced by the grain size of materials and bonding parameters. The metals and alloys with fine grain can be bonded at a lower temperature in the diffusion bonding owing to the better superplasticity [4,5]. This advantage

has been adopted to manufacture the aircraft components with lightweight structures by coupling diffusion bonding and superplastic forming technology [6]. At present, many investigations focus on the influence of bonding parameters on the microstructure and mechanical properties of bond [7–10]. However, the influence of grain size on the void evolution and metallurgical bonding is not deeply discussed, especially on the mechanisms of void evolution and metallurgical bonding.

In this work, the press bonding of Ti–6Al–4V alloy with different grain sizes of primary  $\alpha$  phase was performed. The void evolution and distribution at the bonding interface with different grain sizes were analyzed qualitatively and quantitatively. The variation of the shear strength of bond with grain size of primary  $\alpha$  phase was investigated. The effect of grain size of primary  $\alpha$  phase on the bonding mechanisms was discussed.

## 2 Experimental

The material used in this study is Ti–6Al–4V alloy, of which the chemical composition and the original

microstructure are shown in Table 1 and Fig. 1, respectively. From Fig. 1, it can be seen that the microstructure at room temperature is composed of equiaxed primary  $\alpha$  phase with a grain size of about 8.2  $\mu\text{m}$ , few secondary (platelet)  $\alpha$  phase and a small amount of intergranular  $\beta$  phase. In order to obtain different grain sizes of primary  $\alpha$  phase, the as-received Ti–6Al–4V alloy was heat-treated according to the process shown in Table 2. The measured grain sizes of primary  $\alpha$  phase of heat-treated Ti–6Al–4V alloy are listed in Table 2.

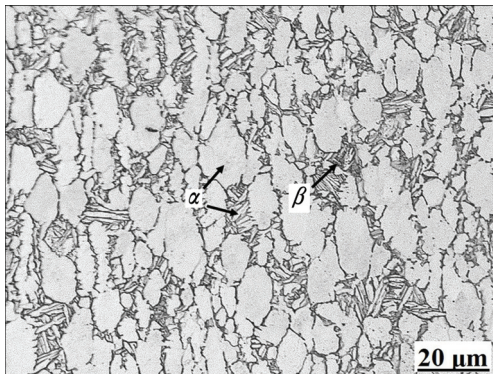


**Fig. 1** Optical micrograph of original microstructure of as-received Ti–6Al–4V alloy

**Table 1** Chemical composition of as-received Ti–6Al–4V alloy (mass fraction, %)

Al	V	Fe	Si	C	N	O	H	Ti
6.05	4.32	0.22	<0.04	0.024	0.006	0.16	0.003	Bal.

**Table 2** Grain sizes of primary  $\alpha$  phase of heat-treated Ti–6Al–4V alloy

No.	Heat treatment process	Grain size of primary $\alpha$ phase/ $\mu\text{m}$
1	(930 °C, 2 h) furnace cooling (FC); (650 °C, 2 h), air cooling (AC)	9.8
2	(930 °C, 12 h), FC; (650 °C, 2 h), AC	12.5
3	(930 °C, 48 h), FC; (650 °C, 2 h), AC	16.4

The specimens for press bonding were in the form of cylindrical blocks of 30.0 mm in diameter and 20.0 mm in height. Before press bonding, the surfaces of specimens to bond were ground by using 1000 grit SiC paper to remove the machining marks and oxidation film. The ground specimens were cleaned ultrasonically in ethanol for 10 min and then dried.

Two ground specimens with the same grain size of primary  $\alpha$  phase were assembled together and then put into a vacuum hot press. They were heated to a temperature of 850 °C at a heating rate of 15 °C/min as

the vacuum degree was up to  $5 \times 10^{-3}$  Pa. After the temperature of the specimens was homogenous, a pressure of 30 MPa was applied to the specimens and kept for 10 min. As the press bonding was completed, the pressure was released and the bonded specimens were cooled in furnace to room temperature.

The height  $h_0$  (mm) of assembled specimens before press bonding and the height  $h$  (mm) of bonded specimens after press bonding were measured by vernier calipers. The deformation ratio ( $e$ ) was proposed to denote the macroscopic plastic deformation of Ti–6Al–4V alloy in the press bonding, which can be calculated as follows:

$$e = (h_0 - h) / h_0 \times 100\% \quad (1)$$

The cross sections of bonded specimens were prepared by standard metallographic method. The bonding interface characteristic was investigated on a TESCAN MIRA3 XMU scanning electron microscope (SEM). The void size was measured by Image-Pro Plus software, which was denoted by the maximum linear length of void along the direction of bonding interface [11]. The bonding ratio was considered as a ratio of the length of bonding interface free of void to the length of the whole bonding interface.

The shear tests of bond and base alloy were conducted on an INSTRON 3382 universal test machine with a crosshead speed of 1.0 mm/min. The geometry of shear test samples is illustrated in Fig. 2. The arrows and dash-dot-line present the direction of shearing force and shear plane, respectively. The shear plane located at the bonding interface. The morphologies of shear fracture surfaces were observed on TESCAN MIRA3 XMU SEM.

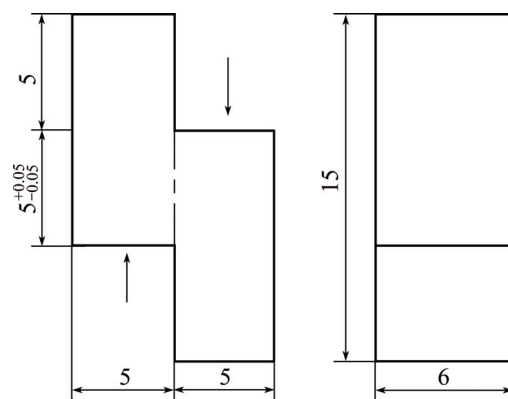


**Fig. 2** Geometry of shear test sample (unit: mm)

## 3 Results

### 3.1 Morphology of bonding interface

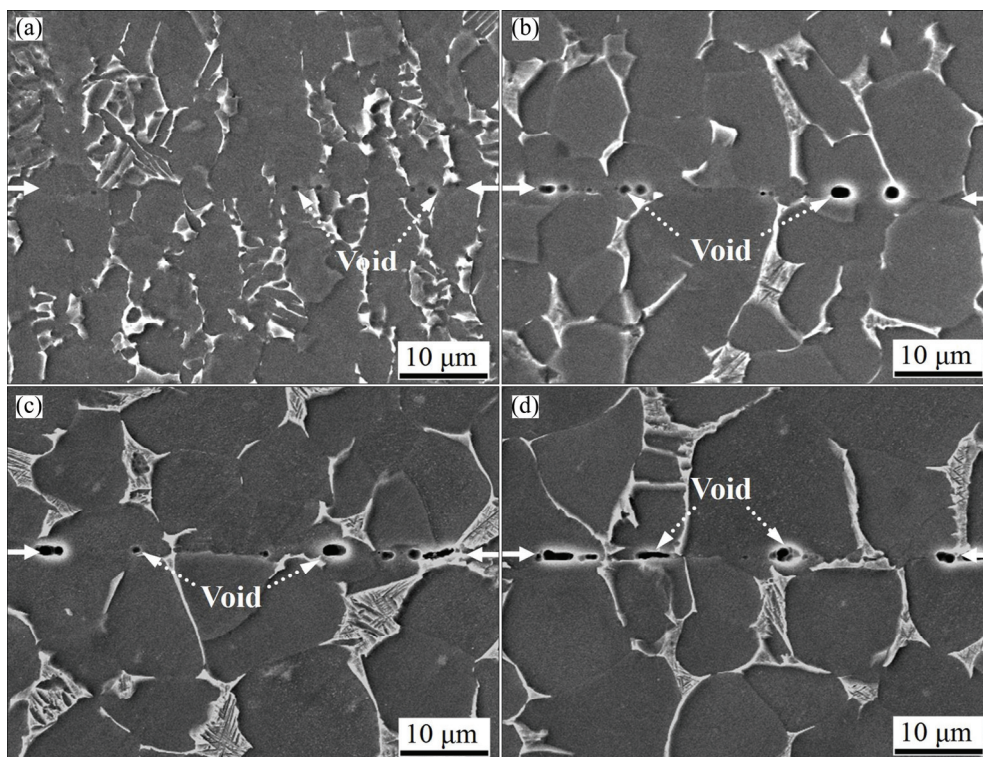
The effect of grain size of primary  $\alpha$  phase of Ti–6Al–4V alloy on the morphology of bonding

interface is shown in Fig. 3. The solid arrows indicate the bonding interface. It can be seen that the effect of grain size of primary  $\alpha$  phase on the morphology of bonding interface is significant at given bonding parameters. As the grain size of primary  $\alpha$  phase is 8.2  $\mu\text{m}$ , the bonding line nearly disappears as shown in Fig. 3(a). There are only a few tiny voids in the shape of round with a smooth edge. The microstructure in some parts of bonding interface free of voids is difficult to identify from that of the base alloy, which demonstrates that a favorable metallurgical bonding has formed in these parts. As the grain size of primary  $\alpha$  phase is 9.8  $\mu\text{m}$ , some voids are left at the bonding interface as seen from Fig. 3(b). The void size increases and the shapes of some voids tend to be ellipse although the edges of voids are still smooth. In Fig. 3(c), there are some tiny round voids and a few bigger voids in the shape of ellipse and strip distributing at the bonding interface of Ti–6Al–4V alloy with a grain size of primary  $\alpha$  phase of 12.5  $\mu\text{m}$ . As the grain size of primary  $\alpha$  phase increases to 16.4  $\mu\text{m}$ , the bonding interface is clear and the void size increases evidently. Most of voids at the bonding interface take the shape of strip with an irregular and wavy edge. The variation of the morphology of bonding interface with grain size of primary  $\alpha$  phase demonstrates that the smaller grain size of primary  $\alpha$  phase of Ti–6Al–4V alloy is beneficial to the closure of voids and formation of bonding interface free of voids.

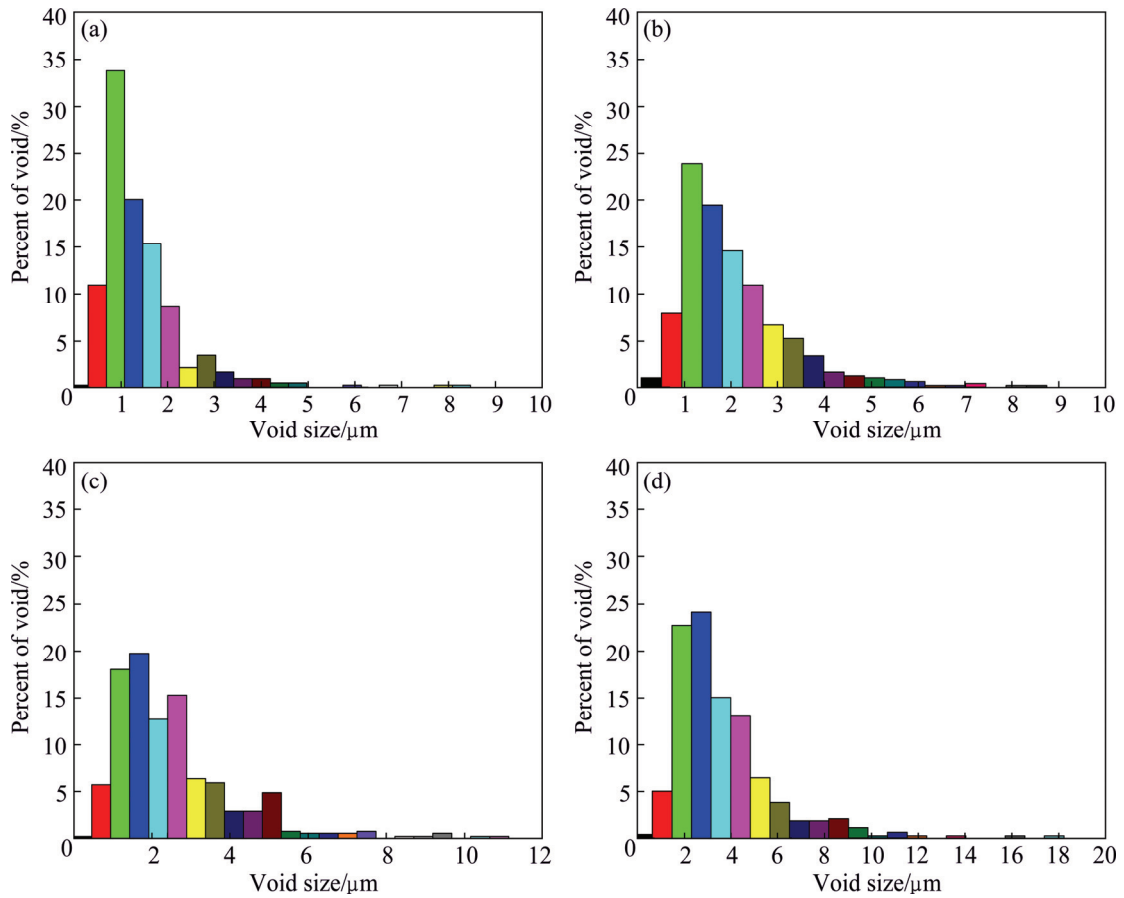
### 3.2 Void size and bonding ratio

Figure 4 shows the distribution of void size at the bonding interface of Ti–6Al–4V alloy with different grain sizes of primary  $\alpha$  phase at a temperature of 850  $^{\circ}\text{C}$  and pressure of 30 MPa for 10 min. As seen from Fig. 4(a), there are about 94% voids with a size ranging from 0.1 to 2.8  $\mu\text{m}$  at the bonding interface of Ti–6Al–4V alloy with a grain size of primary  $\alpha$  phase of 8.2  $\mu\text{m}$ , and the maximum void size is only about 8.1  $\mu\text{m}$ . With the increase of grain size of primary  $\alpha$  phase, the percent of voids with a larger size increases and the distribution range of void size tends to be wider. When the grain size of primary  $\alpha$  phase increases to 16.4  $\mu\text{m}$ , the percent of voids with a size exceeding 5.0  $\mu\text{m}$  increases obviously and there are about 97% voids with a size ranging from 0.2 to 9.4  $\mu\text{m}$ . The maximum void size is about 17.3  $\mu\text{m}$ .

The variation of the average size of voids and bonding ratio of Ti–6Al–4V alloy with grain size of primary  $\alpha$  phase is illustrated in Fig. 5. With an increase in grain size of primary  $\alpha$  phase, the average size of voids increases from 0.8 to 2.6  $\mu\text{m}$  while the bonding ratio decreases from 90.9% to 77.8% as the Ti–6Al–4V alloy is bonded at the temperature of 850  $^{\circ}\text{C}$  and pressure of 30 MPa for 10 min. Especially, the variation of the average size of voids and bonding ratio with grain size of primary  $\alpha$  phase ranging from 8.2 to 9.8  $\mu\text{m}$  is more distinct.



**Fig. 3** SEM images of bonding interface of Ti–6Al–4V alloy with different grain sizes of primary  $\alpha$  phase: (a) 8.2  $\mu\text{m}$ ; (b) 9.8  $\mu\text{m}$ ; (c) 12.5  $\mu\text{m}$ ; (d) 16.4  $\mu\text{m}$



**Fig. 4** Distribution of void size at bonding interface of Ti-6Al-4V alloy with different grain sizes of primary  $\alpha$  phase: (a) 8.2  $\mu\text{m}$ ; (b) 9.8  $\mu\text{m}$ ; (c) 12.5  $\mu\text{m}$ ; (d) 16.4  $\mu\text{m}$

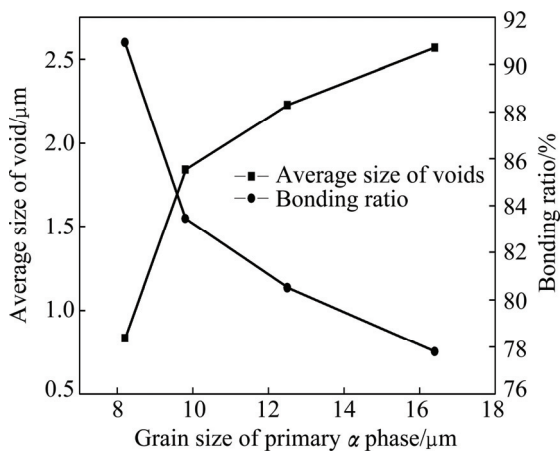


**Fig. 5** Average size of voids and bonding ratio at bonding interface of Ti-6Al-4V alloy with different grain sizes of primary  $\alpha$  phase

### 3.3 Shear strength of bond

Figure 6 shows the shear strength of bond and base alloy of Ti-6Al-4V alloy with different grain sizes of primary  $\alpha$  phase bonded at temperature of 850  $^{\circ}\text{C}$  and pressure of 30 MPa for 10 min. As the grain size of primary  $\alpha$  phase is 8.2  $\mu\text{m}$ , the shear strength of bond is about 761 MPa, which is close to that of base alloy

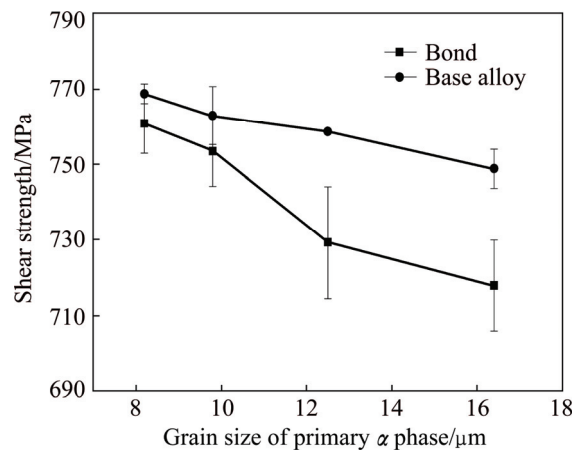


**Fig. 6** Shear strength of bond and base alloy of Ti-6Al-4V alloy with different grain sizes of primary  $\alpha$  phase

about 769 MPa. With an increase in grain size of primary  $\alpha$  phase, the shear strength of bond decreases gradually and that of base alloy decreases slightly. The difference between the shear strength of bond and that of base alloy becomes larger and larger. At the grain size of primary  $\alpha$  phase of 16.4  $\mu\text{m}$ , the shear strength of bond is only about 718 MPa, which is lower than that of the base alloy. It can be concluded that the decrease in shear

strength of bond is resulted from not only lower shear strength of Ti–6Al–4V alloy with larger grain size but also the lower bonding ratio at bonding interface of Ti–6Al–4V alloy with larger grain size.

The shear fracture surface morphologies of Ti–6Al–4V alloy bonds with different grain sizes of primary  $\alpha$  phase can be seen in Fig. 7. At the grain size of primary  $\alpha$  phase of 8.2  $\mu\text{m}$ , the fracture surface is rough on which mass of deep dimples are left as shown in Fig. 7(a). This is a typical feature of ductile fracture which demonstrates the formation of a metallurgical bond with fairly high mechanical property. With an increase in grain size of primary  $\alpha$  phase, the depth of dimple decreases and the area exhibiting dimples on the fracture surface reduces. As seen from Fig. 7(d), there are only few zones exhibiting some small and shallow dimples or tear ridges on the fracture surface of bond as the grain size of primary  $\alpha$  phase is 16.4  $\mu\text{m}$ . Most zones on the fracture surface are smooth which present the uncontacted areas or contacted areas without metallurgical bonding.

#### 4 Discussion

According to the results mentioned above, it is well known that the effect of grain size of primary  $\alpha$  phase on the bonding interface characteristic and mechanical property of bond is significant. The smaller the grain size of primary  $\alpha$  phase is, the higher the bonding ratio and

shear strength of bond are. The press bonding process and mechanisms of Ti–6Al–4V alloy are influenced by grain size of primary  $\alpha$  phase.

The press bonding can be considered as a process composed of two stages. The first stage is that two free bonding surfaces with roughness in microscopic level fit together and then a physical interface free of voids forms. This stage can be described as a process of void closure, which is determined by the mass transfer resulted from mechanisms of plastic flow and diffusion [12]. These mechanisms are strongly influenced by grain size of primary  $\alpha$  phase. Figure 8 shows the variation of the deformation ratio of Ti–6Al–4V alloy with grain size of primary  $\alpha$  phase in the press bonding. It can be seen from Fig. 8 that the deformation ratio of Ti–6Al–4V alloy decreases from 12.7% to 3.3% as the grain size of primary  $\alpha$  phase increases from 8.2 to 16.4  $\mu\text{m}$ . This phenomenon indicates that the ability of plastic flow at high temperature is limited in the Ti–6Al–4V alloy with a larger grain size of primary  $\alpha$  phase. Some investigations published in literatures demonstrate that the ability of plastic deformation denoted by the strain rate sensitivity or elongation increases with decreasing grain size at elevated temperatures [13,14]. This is because the grain boundary sliding plays an important role in the elevated temperature plastic deformation of Ti–6Al–4V alloy and there are more grain boundaries in this alloy with smaller grain size of primary  $\alpha$  phase. Meanwhile, the grain boundary sliding is also the

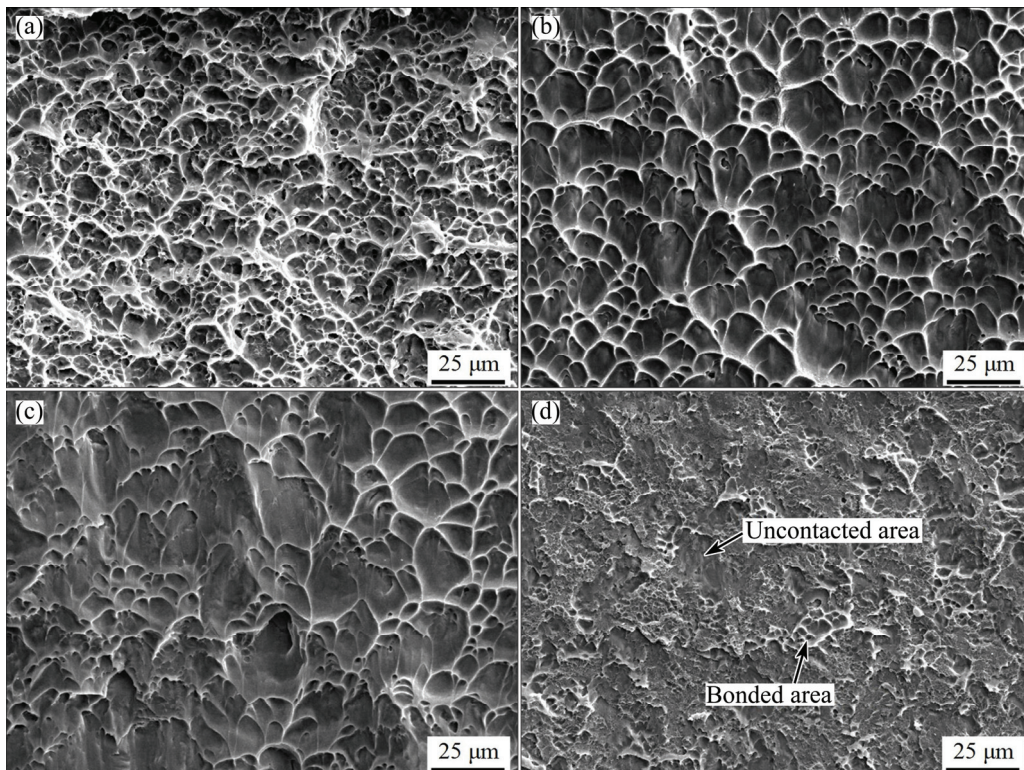


**Fig. 7** SEM images of shear fracture surface of Ti–6Al–4V alloy bonds with different grain sizes of primary  $\alpha$  phase: (a) 8.2  $\mu\text{m}$ ; (b) 9.8  $\mu\text{m}$ ; (c) 12.5  $\mu\text{m}$ ; (d) 16.4  $\mu\text{m}$

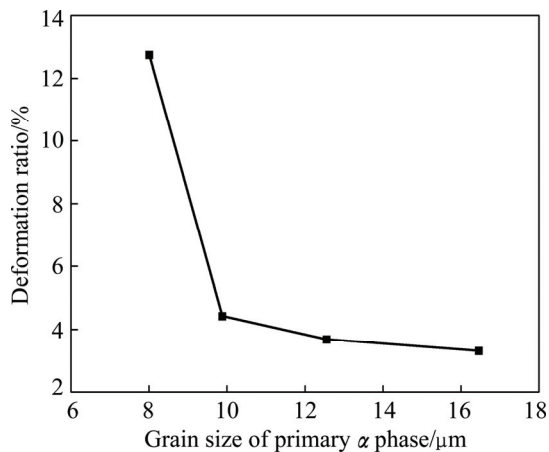


**Fig. 8** Variation of deformation ratio of Ti-6Al-4V alloy with grain size of primary  $\alpha$  phase

dominant mechanism in the creep of Ti-6Al-4V alloy. Moreover, the diffusion is an important mechanism in the creep of metals and alloys. As the grain sizes are smaller, the grain boundaries to participate in atom diffusion are more and the diffusion paths are shorter. A higher creep rate can be obtained in metals and alloys with a smaller grain size [15,16]. In summary, the enhanced ability of plastic flow will promote the process of void closure. Figure 9 shows the variation of the average size of voids and the bonding ratio with the deformation ratio of Ti-6Al-4V alloy. It can be seen from Fig. 9 that the average size of voids decreases and bonding ratio increases evidently with the increase of deformation ratio of Ti-6Al-4V alloy. The similar result can be obtained in the press bonding of Ti-17 alloy as shown in Ref. [3]. In addition, more grain boundaries in the Ti-6Al-4V alloy with a smaller grain size of primary  $\alpha$  phase will provide more and shorter direct paths of mass transfer to void.

The second stage is the formation of bond with metallurgical structure at the bonding interface free of

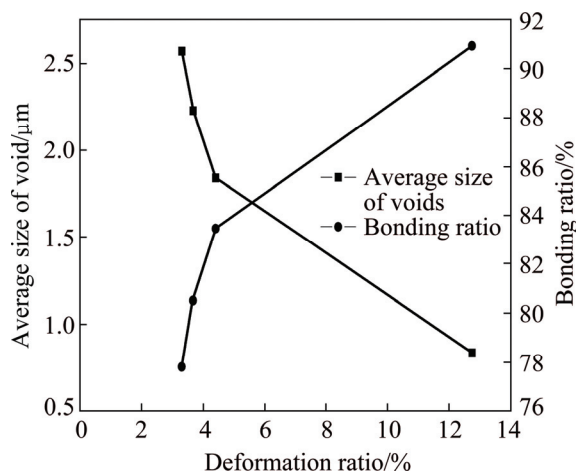


**Fig. 9** Variation of average size of voids and bonding ratio with deformation ratio of Ti-6Al-4V alloy

voids. In this stage, the disappearance of original bonding interface is essential for achieving a high strength bond. The grains at the bonding interface of Ti-6Al-4V alloy with different grain sizes of primary  $\alpha$  phase can be seen in Fig. 10. The arrows present the original bonding interface. In Fig. 10(a), the original bonding interface is rarely identified and the  $\alpha$  grains and continuous  $\beta$  phase across the original bonding interface denoted by dashed curves can be clearly observed as the grain size of primary  $\alpha$  phase of Ti-6Al-4V alloy is 8.2  $\mu\text{m}$ . However, the original bonding interface can be seen clearly in Fig. 10(b) and it is nearly in a straight line presented in a dashed curve as the grain size of primary  $\alpha$  phase of Ti-6Al-4V alloy is 16.4  $\mu\text{m}$ . The disappearance of original bonding interface can also be seen in the press/diffusion bonding of Ti-17 alloy [3], TC21 alloy [17], copper [18] and steel [19], which is usually attributed to the migration of the interfacial grain boundary from the interface. In Ti-6Al-4V alloy with smaller grain size of primary  $\alpha$  phase, the higher diffusion capability and larger strain at given bonding parameters will promote the migration of the interfacial grain boundary compared with that in Ti-6Al-4V alloy with larger grain size of primary  $\alpha$  phase. Therefore, a bond with higher shear strength can be easily obtained in the Ti-6Al-4V alloy with smaller grain size of primary  $\alpha$  phase at given bonding parameters.

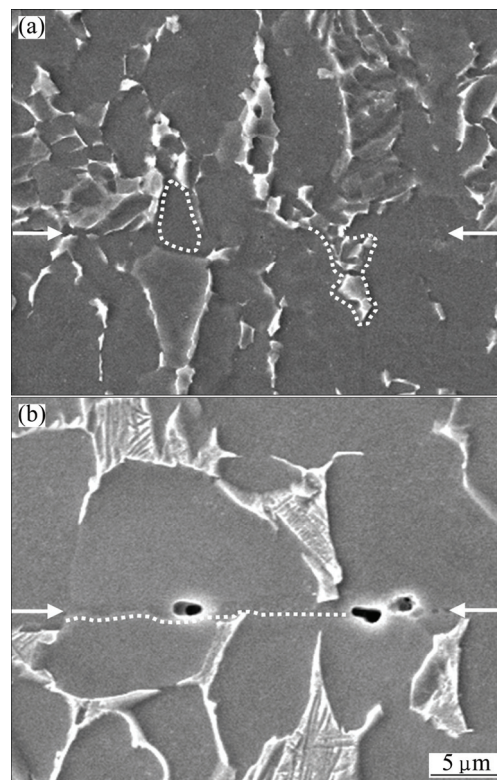


**Fig. 10** SEM images of bonding interface of Ti-6Al-4V alloy with different grain sizes of primary  $\alpha$  phase: (a) 8.2  $\mu\text{m}$ ; (b) 16.4  $\mu\text{m}$

## 5 Conclusions

1) With the increase in grain size of primary  $\alpha$  phase from 8.2 to 16.4  $\mu\text{m}$ , the average size of voids increases from 0.8 to 2.6  $\mu\text{m}$  and the bonding ratio decreases from 90.9% to 77.8%. The shape of voids left at the bonding interface changes from the tiny round to the irregular strip.

2) With the increase in grain size of primary  $\alpha$  phase from 8.2 to 16.4  $\mu\text{m}$ , the shear strength of bond decreases from 761 to 718 MPa and that of base alloy decreases from 769 to 749 MPa. The area exhibiting dimples reduces and the depth of dimple decreases on the fracture surface.

3) The smaller grain size of primary  $\alpha$  phase demonstrates higher ability of plastic flow and diffusion, which promotes the process of void closure and formation of  $\alpha/\beta$  grains across the original bonding interface in the press bonding of Ti–6Al–4V alloy.

## References

- [1] ATIEH A M, KHAN T I. Effect of process parameters on semi-solid TLP bonding of Ti–6Al–4V to Mg–AZ31 [J]. Journal of Materials Science, 2013, 48: 6737–6745.
- [2] MOISEYEV V N. Titanium alloys: Russian aircraft and aerospace applications [M]. FL: Taylor & Francis Group, 2006.
- [3] LI H, LIU H B, YU W X, LI M Q. Fabrication of high strength bond of Ti–17 alloy using press bonding under a high bonding pressure [J]. Materials Letters, 2013, 108: 212–214.
- [4] SALISHCHEV G A, GALEYEV R M, VALIAKHMETOV O R, SAFIULLIN R V, LUTFULLIN R Y, SENKOV O N, FROES F H, KAIBYSHEV O A. Development of Ti–6Al–4V sheet with low temperature superplastic properties [J]. Journal of Materials Processing Technology, 2001, 116: 265–268.
- [5] KAIBYSHEV O A, SAFIULLIN R V, LUTFULLIN R Y, VALIAKHMETOV O R, GALEYEV R M, DUTTA A, RAGHU T, SAHA G G. Advanced superplastic forming and diffusion bonding of titanium alloy [J]. Materials Science and Technology, 2006, 22(3): 343–348.
- [6] HEFTI L D. Innovations in the superplastic forming and diffusion bonded process [J]. Journal of Materials Engineering and Performance, 2008, 17(2): 178–182.
- [7] CALVO F A, GÓMEZ DE SALAZAR J M, UREÑA A, CARRIÓN J G, PEROSANZ F. Diffusion bonding of Ti–6Al–4V alloy at low temperature: Metallurgical aspects [J]. Journal of Materials Science, 1992, 27(2): 391–398.
- [8] GÓMEZ DE SALAZAR J M, UREÑA A, CARRIÓN J G. Charpy impact test of Ti–6Al–4V joints diffusion welded at low temperature [J]. Scripta Materialia, 1996, 35: 479–484.
- [9] LEE H S, YOON J H, PARK C H, KO Y G, SHIN D H, LEE C S. A study on diffusion bonding of superplastic Ti–6Al–4V ELI grade [J]. Journal of Materials Processing Technology, 2007, 187–188: 526–529.
- [10] RAYUDU R K, ARUNKUMAR T, BHATTACHARYA S S. Experimental studies on the superplastic forming of square shaped components and diffusion bonding characteristics of Ti–6Al–4V alloy [J]. Transactions of the Indian Institute of Metals, 2013, 66(4): 313–323.
- [11] LI Hong, ZHANG Chao, LIU Hong-bin, LI Miao-quan. Bonding interface characteristic and shear strength of diffusion bonded Ti–17 titanium alloy [J]. Transactions of Nonferrous Metals Society of China, 2015, 25(1): 80–87.
- [12] DERBY B, WALLACH E R. Theoretical model for diffusion bonding [J]. Metal Science, 1982, 16(1): 49–56.
- [13] KORLA R, CHOKSHI A H. Strain-rate sensitivity and microstructural evolution in a Mg–Al–Zn alloy [J]. Scripta Materialia, 2010, 63: 913–916.
- [14] WOO K D, KIM S W, YANG C H, LOU T P, MIURA Y. Effects of grain size on high temperature deformation behavior of Al–4Mg–0.4Sc alloy [J]. Materials Letters, 2003, 57: 1903–1909.
- [15] MARUYAMA K, YAMAMOTO R, NAKAKUKI H, FUJITSUNA N. Effects of lamellar spacing, volume fraction and grain size on creep strength of fully lamellar TiAl alloys [J]. Materials Science and Engineering A, 1997, 239–240: 419–428.
- [16] NING Z L, LIU H H, CAO F Y, WANG S T, SUN J F, QIAN M. The effect of grain size on the tensile and creep properties of Mg–2.6Nd–0.35Zn–xZr alloys at 250 °C [J]. Materials Science and Engineering A, 2013, 560: 163–169.
- [17] LIU Hui-jie, FENG Xiu-li. Microstructures and interfacial quality of diffusion bonded TC21 titanium alloy joints [J]. Transactions of Nonferrous Metals Society of China, 2011, 21(1): 58–64.
- [18] MARTINEZ M, LEGROS M, SIGNAMARCHEIX T, BALLY L, VERRUN S, CIOCCIO L D, DEGNET C. Mechanisms of copper direct bonding observed by in-situ and quantitative transmission electron microscopy [J]. Thin Solid Films, 2013, 530: 96–99.
- [19] ZHANG C, LI H, LI M Q. Formation mechanisms of high quality diffusion bonded martensitic stainless steel joints [J]. Science and Technology of Welding and Joining, 2015, 20(2): 115–122.

# 初生 $\alpha$ 相晶粒尺寸对 Ti–6Al–4V 合金 压力连接界面特征及力学性能的影响

李宏<sup>1,2</sup>, 李淼泉<sup>1,2</sup>, 刘宏彬<sup>2</sup>, 张超<sup>2</sup>

1. 西北工业大学 凝固技术国家重点实验室, 西安 710072; 2. 西北工业大学 材料学院, 西安 710072

**摘要:** 研究初生  $\alpha$  相晶粒尺寸对 Ti–6Al–4V 合金压力连接界面特征及接头剪切强度的影响。定量试验结果表明, 当初生  $\alpha$  相晶粒尺寸由 8.2  $\mu\text{m}$  增大至 16.4  $\mu\text{m}$  时, 平均空洞尺寸由 0.8  $\mu\text{m}$  增大至 2.6  $\mu\text{m}$ , 连接率由 90.9% 降至 77.8%。空洞形状由微小的圆形转变为不规则的条状。初生  $\alpha$  相晶粒尺寸为 8.2  $\mu\text{m}$  的 Ti–6Al–4V 合金压力连接接头剪切强度最高。这是因为初生  $\alpha$  相晶粒尺寸越小, Ti–6Al–4V 合金塑性流动能力越强, 短程扩散通道越多, 从而促进了空洞闭合和跨连接界面的  $\alpha/\beta$  晶粒的形成。

**关键词:** 晶粒尺寸; 连接界面; 空洞闭合; 剪切强度; 压力连接; Ti–6Al–4V 合金

(Edited by Xiang-qun LI)